

# Ghrelin modulates the activity and synaptic input organization of midbrain dopamine neurons while promoting appetite

Alfonso Abizaid,<sup>1</sup> Zhong-Wu Liu,<sup>1,2</sup> Zane B. Andrews,<sup>1</sup> Marya Shanabrough,<sup>1</sup> Erzsebet Borok,<sup>1</sup> John D. Elsworth,<sup>3,4</sup> Robert H. Roth,<sup>3,4</sup> Mark W. Sleeman,<sup>5</sup> Marina R. Picciotto,<sup>4,6</sup> Matthias H. Tschöp,<sup>7</sup> Xiao-Bing Gao,<sup>1</sup> and Tamas L. Horvath<sup>1,6,8</sup>

<sup>1</sup>Department of Obstetrics, Gynecology, and Reproductive Sciences, Yale University School of Medicine, New Haven, Connecticut, USA.

<sup>2</sup>Department of Neurobiology, Yongyang Medical College, Hubei, China. <sup>3</sup>Department of Pharmacology and <sup>4</sup>Department of Psychiatry, Yale University School of Medicine, New Haven, Connecticut, USA. <sup>5</sup>Regeneron Inc., Tarrytown, New York, USA. <sup>6</sup>Department of Neurobiology, Yale University School of Medicine, New Haven, Connecticut, USA. <sup>7</sup>Department of Psychiatry, University of Cincinnati, Cincinnati, Ohio, USA.

<sup>8</sup>Section of Comparative Medicine, Yale University School of Medicine, New Haven, Connecticut, USA.

**The gut hormone ghrelin targets the brain to promote food intake and adiposity. The ghrelin receptor growth hormone secretagogue 1 receptor (GHSR) is present in hypothalamic centers controlling energy metabolism as well as in the ventral tegmental area (VTA), a region important for motivational aspects of multiple behaviors, including feeding. Here we show that in mice and rats, ghrelin bound to neurons of the VTA, where it triggered increased dopamine neuronal activity, synapse formation, and dopamine turnover in the nucleus accumbens in a GHSR-dependent manner. Direct VTA administration of ghrelin also triggered feeding, while intra-VTA delivery of a selective GHSR antagonist blocked the orexigenic effect of circulating ghrelin and blunted rebound feeding following fasting. In addition, ghrelin- and GHSR-deficient mice showed attenuated feeding responses to restricted feeding schedules. Taken together, these data suggest that the mesolimbic reward circuitry is targeted by peripheral ghrelin to influence physiological mechanisms related to feeding.**

## Introduction

Ghrelin is a 28-amino acid peptide that regulates growth hormone secretion, food intake, and energy homeostasis (1–3). It is thought that ghrelin targets specific neuronal subpopulations within hypothalamic sites, particularly the arcuate nucleus (ARC), in producing these effects (4). For example, ghrelin modulates the activity of neuropeptide Y and melanocortin neurons in exerting a potent orexigenic effect (4–7). The colocalization of the growth hormone secretagogue 1 receptor (GHSR; the only known receptor for ghrelin) with these hypothalamic neurons further indicates that the hypothalamus is a main target site for ghrelin (8–10). Interestingly, the presence of the transcripts encoding the GHSR message has been detected in various extrahypothalamic brain regions as well, including the ventral tegmental area (VTA) (11, 12).

The mesolimbic dopaminergic system, located in the VTA, plays an important role in the mechanisms underlying reward-seeking behavior, including behaviors conducted to obtain natural rewards like food (13, 14). The activity of this system is associated with the experience or the expectation of reward and exposure to pleasurable stimuli (13, 15, 16). Palatable foods, sexual experience, or drugs of abuse all result in an increase in dopamine (DA) release from neurons in the VTA and the adjacent substantia nigra into forebrain structures like the nucleus accumbens and the striatum.

In addition, pharmacologic modulation of neurotransmitter systems in these regions produces changes in food intake (reviewed in refs. 17–19). Based on this model, and inspired by the abundance of GHSR message in these regions (11, 12), we examined the potential role of ghrelin in directly modulating the activity of the mesolimbic dopaminergic system.

Our results revealed that ghrelin bound to VTA neurons and that GHSRs were expressed in dopaminergic and GABAergic neuronal subpopulations. Ghrelin increased the firing rate of VTA DA neurons, promoted recruitment of asymmetric synapses onto dopaminergic perikarya, and increased DA turnover in the nucleus accumbens, the major target of the VTA. Selective administration of ghrelin or its antagonist altered food intake, and ghrelin- and GHSR-deficient mice had attenuated feeding responses in a feeding paradigm where animals had access to food for only a few hours a day. Taken together, our data suggest that the mesolimbic reward circuitry is a target of ghrelin in the physiological regulation of feeding.

## Results

*The VTA is a target for ghrelin.* To determine whether ghrelin binds to cells of this mesolimbic area, we studied ghrelin binding on rat brain slices containing the VTA using a previously described protocol (5). Biotinylated ghrelin binding was present in the rat VTA with a distribution pattern similar to that of GHSR immunolabeled cells (see below). Ghrelin binding was most robust in the vicinity of neuronal perikarya, a labeling that was not observed when unlabeled ghrelin was used in the incubating solution (Figure 1, A–C). These observations strengthen the possibility that ghrelin may have a direct effect on VTA neuronal activity.

To confirm that ghrelin can act directly in the VTA, we analyzed GHSR protein expression in this area. Consistent with previous

**Nonstandard abbreviations used:** AP5, R-2-amino-5-phosphonopentanoate; ARC, arcuate nucleus; CNQX, 6-cyano-7-nitro-quininoxaline-2,3-dione; DA, dopamine; DOPAC, dihydroxyphenylacetic acid; GHSR, growth hormone secretagogue 1 receptor; mIPSC, miniature inhibitory postsynaptic current; mEPSC, miniature excitatory postsynaptic current; PB, phosphate buffer; TH, tyrosine hydroxylase; vGlut2, vesicular glutamate transporter 2; VTA, ventral tegmental area.

**Conflict of interest:** The authors have declared that no conflict of interest exists.

**Citation for this article:** *J. Clin. Invest.* 116:3229–3239 (2006). doi:10.1172/JCI29867.

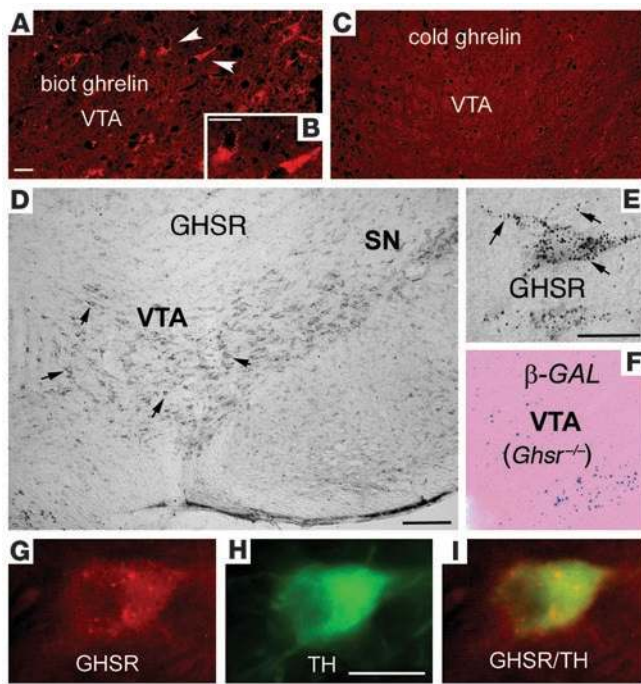


**Figure 1**  
 Expression of GHSR and ghrelin binding in VTA neurons of the rat. (A–C) Rat VTA sections incubated in either biotinylated (biot) ghrelin (arrowheads; A and B) or unlabeled (cold) ghrelin (C). (D and E) GHSR immunocytochemistry in mouse (D) and rat (E) brain sections. Dense immunolabeling was observed in the VTA (D, arrows), with cells showing bouton-like immunoreactivity (IR; E, arrows). SN, substantia nigra. (F)  $\beta$ -Gal-labeled blue nuclei in the VTA of *Ghsr*<sup>-/-</sup> mice confirmed expression of GHSR. (G–I) High-magnification images of a GHSR-immunolabeled (red) cell that coexpressed TH (green). Scale bars: 10  $\mu$ m (A–C, E, and G–I); 100  $\mu$ m (D and F).

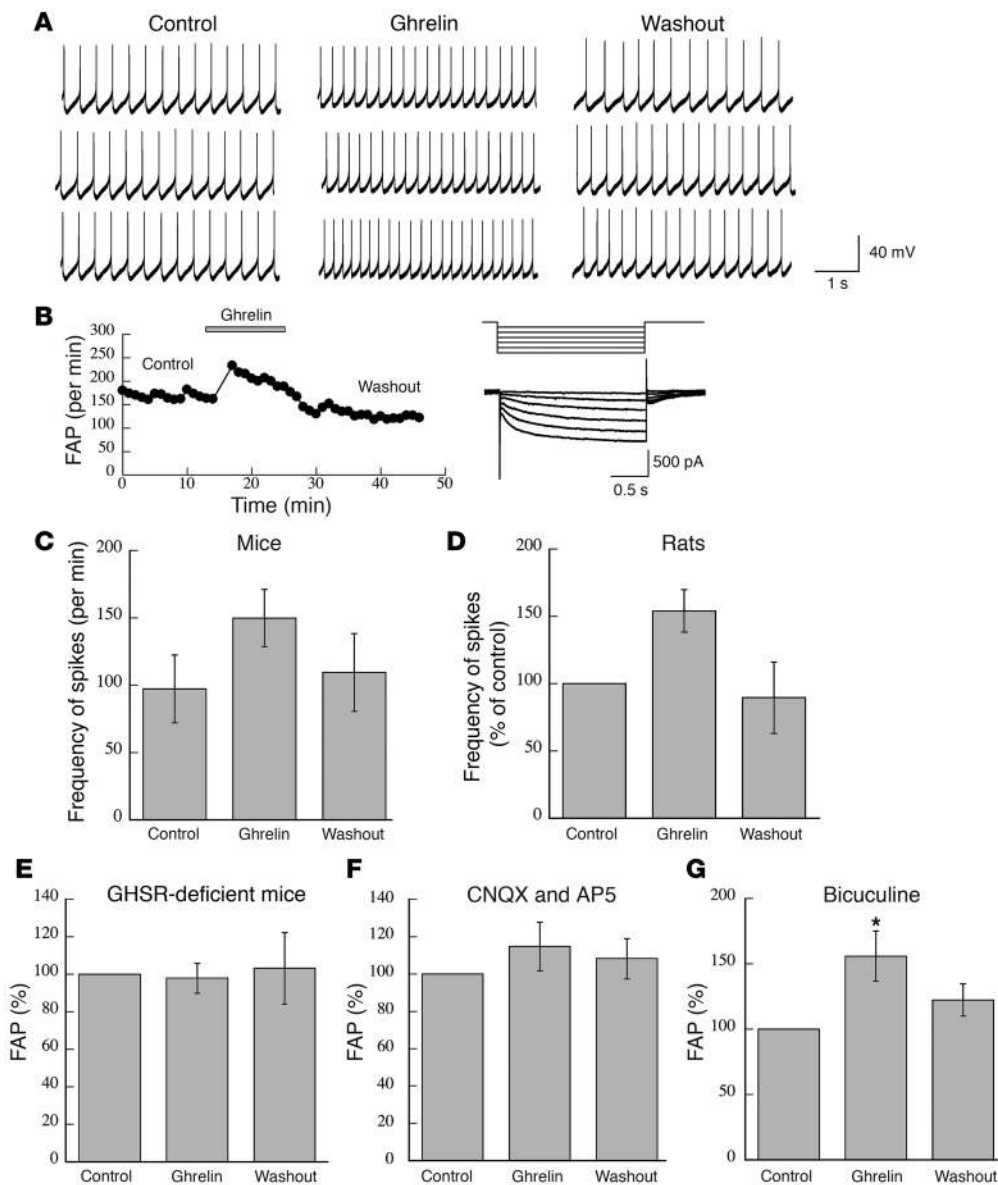
descriptions of GHSR mRNA distribution (11, 12), GHSR immunoreactivity was detected in neurons throughout the rostrocaudal extent of the VTA and substantia nigra of mice and rats (Figure 1, D and E). The immunolabeling was predominantly associated with putative pre- or postsynaptic profiles, which is consistent with previous demonstrations of both pre- and postsynaptic actions of ghrelin in the hypothalamus (5). No immunostaining was observed in tissue obtained from *Ghsr*<sup>-/-</sup> mice (data not shown), while these animals expressed *LacZ*, a transcript that replaced the *Ghsr* gene, in the VTA as revealed by  $\beta$ -gal labeling (Figure 1F). Double-labeling studies in rats and mice revealed that GHSR immunoreactivity was present in about 60% of VTA DA neurons (Figure 1, G–I) and about 30% of VTA GABA cells (data not shown), the 2 dominant cell types of this region. A closer examination of the sections revealed that colocalization of GHSR immunoreactivity with DA was highest in the anterior portion of the VTA of rats (5.0–5.3 mm caudal to bregma).

*Ghrelin increases the activity of dopaminergic cells in the VTA of rats and mice.* We next analyzed whether ghrelin directly influences the electrophysiologic responses of VTA DA cells. Whole-cell patch clamp recordings were performed in DA neurons in the VTA in rat ( $n = 5$ ) and mouse ( $n = 9$ ) brain slices (Figure 2A). DA neurons under electrophysiologic examination were within the boundaries of the VTA and were identified based on their characteristic

Th current (refs. 20–22; see Methods for further details). Spontaneous action potentials were recorded under current clamp. After at least 10 minutes of stable recording of action potentials, 0.5–3  $\mu$ M ghrelin was applied to the recorded DA neurons via bath application (Figure 2B). In mice, in 5 of 7 cells the frequency of action potentials significantly increased from  $97.2 \pm 25.2$  per minute to  $149.8 \pm 21.3$  per minute in the presence of ghrelin ( $t_4 = 3.79$ ,  $P < 0.05$ ) and returned to  $109.5 \pm 29.0$  per minute after its withdrawal. In rats, baseline frequency of action potentials was  $153.24 \pm 45$  spikes per minute. In 4 of 6 cells, the recorded action potential frequency was  $154.0\% \pm 15.9\%$  higher than baseline in the presence of ghrelin and  $89.6\% \pm 26.3\%$  of controls after its withdrawal (Figure 2D). The ghrelin-induced increase in the frequency of action potentials was significant ( $t_3 = -3.40$ ,  $P < 0.05$ ). Thus, our data provide electrophysiologic evidence that ghrelin promotes the generation of action potentials in most (but not all) DA neurons of the VTA of both mice and rats.

To further verify the effect of ghrelin on the frequency of action potentials in DA neurons in the VTA, *Ghsr*<sup>-/-</sup> mice were used. In slices prepared from *Ghsr*<sup>-/-</sup> mice, the frequency of action potentials was  $97.8\% \pm 8.0\%$  of control ( $n = 5$ ) in the presence of ghrelin and  $103.2\% \pm 19.0\%$  of control after withdrawal of ghrelin (Figure 2E). The application of ghrelin did not induce any change in the frequency of action potentials in all tested neurons ( $F_{2,14} = 0.034$ ,  $P > 0.05$ ). Next, we further explored the mechanism of ghrelin-mediated effect on action potentials in DA neurons. In the presence of ionotropic glutamate receptor antagonists 6-cyano-7-nitro-quininoxaline-2,3-dione (CNQX; 10  $\mu$ M) and R-2-amino-5-phosphonopentanoate (AP5; 50  $\mu$ M) in all solutions, the frequency of action potentials was  $114.8\% \pm 12.9\%$  of control ( $n = 6$ ) in the presence of ghrelin and  $108.2\% \pm 10.8\%$  of control after withdrawal of ghrelin (Figure 2F). Thus, in the absence of presynaptic excitatory input, ghrelin was unable to activate VTA DA neurons ( $F_{2,17} = 0.58$ ,  $P > 0.05$ ). In contrast, in the presence of GABA<sub>A</sub> receptor antagonist bicuculline (30  $\mu$ M; used to block GABA effects) in all solutions, the frequency of action potentials was  $155.9\% \pm 19.3\%$  of control ( $n = 7$ ) in the presence of ghrelin and  $122.3\% \pm 12.4\%$  of control after withdrawal of ghrelin (Figure 2G). Thus, ghrelin still significantly increased the frequency of action potentials in all tested DA neurons when GABAergic synaptic transmission was blocked ( $F_{2,21} = 4.52$ ,  $P < 0.05$ ). Our data suggest that the ghrelin-mediated increment in the frequency of action potentials in DA neurons requires excitatory inputs to these neurons.

*Ghrelin alters the synaptic wiring of mouse mesolimbic DA cells.* In contrast to the above electrophysiologic observations, ghrelin was previously found to act on hypothalamic pro-opiomelanocortin neurons mediated by presynaptic GABA input (5). In that system, the presynaptic promotion of GABA transmission was then associated with initiation of synaptic plasticity by ghrelin, resulting in a synaptic balance on pro-opiomelanocortin neurons that was dominated by GABA inputs (23). Thus, we sought to determine whether the VTA effects of ghrelin via excitatory inputs may also underlie synaptic rearrangement of DA neurons, particularly because synaptic plasticity within the VTA has been associated with reward-seeking behaviors (24). Mice were injected i.p. with either ghrelin (100  $\mu$ g) in saline or saline alone as vehicle ( $n = 5$  per group). Ninety minutes later, animals were anesthetized and killed by transcardial perfusion, and their brains were processed for tyrosine hydroxylase (TH) immunocytochemistry and electron microscopy analysis of synapses as described previously (23) as well as for double-labeling

**Figure 2**

Ghrelin increases action potential generation in VTA DA neurons in mice ( $n = 9$ ) and rats ( $n = 6$ ). **(A)** Raw traces recorded before (Control), during (Ghrelin), and after (Washout) application of ghrelin. **(B)** Time course of the ghrelin-induced increase in frequency of action potential (FAP). **A–C** represent time points when traces from **A** were recorded. **(C and D)** Mean frequency of action potentials recorded in mice **(C)** and rats **(D)** before, during, and after application of ghrelin. Hyperpolarization-induced action current recorded from DA neurons is shown **(D, inset)**. **(E and F)** Ghrelin-mediated enhancement of action potential generation in VTA DA neurons required excitatory inputs. Shown are mean frequency of action potentials recorded before, during, and after application of ghrelin. **(E)** No effect of ghrelin was observed on frequency of action potentials in slices from GHSR-knockout mice ( $n = 5$ ). **(F)** In the absence of excitatory input onto DA neurons, no effect of ghrelin was observed on frequency of action potentials in slices from wild-type mice ( $n = 6$ ) in the presence of CNQX (10  $\mu\text{M}$ ) and AP5 (50  $\mu\text{M}$ ) in all solutions. Results were pooled from all recorded neurons. **(G)** Experiments were performed in slices from wild-type mice ( $n = 7$ ) in the presence of bicuculline (30  $\mu\text{M}$ ) in all solutions. Results were pooled from all recorded neurons. In the absence of inhibitory inputs of DA neurons, ghrelin elevated the frequency of action potentials of VTA DA neurons, an effect that diminished after washout.

fluorescence microscopy to detect putative contact between excitatory (vesicular glutamate transporter 2-immunopositive [vGlut2-immunopositive]) or inhibitory (GAD-67 immunopositive) inputs onto TH-immunoreactive cells. Synapses and putative contacts

were analyzed on 10 randomly selected VTA TH-immunoreactive perikarya of each animal.

The total number of synapses on TH-immunolabeled perikarya was elevated by ghrelin administration ( $15.41 \pm 2.04$  versus  $10.15 \pm 1.71$  synapses/100  $\mu\text{m}$  perikaryal membrane;  $t_9 = 2.92$ ,  $P = 0.06$ ; Figure 3). Further analysis revealed that there was a robust elevation in the number of asymmetric, putatively excitatory synapses ( $14.07 \pm 2.28$  versus  $3.23 \pm 0.99$  synapses/100  $\mu\text{m}$  perikaryal membrane;  $t_9 = 4.46$ ,  $P < 0.01$ ; Figure 3), while symmetric, putatively inhibitory contacts were reduced after ghrelin treatment ( $1.325 \pm 0.46$  versus  $6.892 \pm 1.85$  synapses/100  $\mu\text{m}$  perikaryal membrane;  $t_9 = -3.55$ ,  $P < 0.01$ ; Figure 3). No synaptic changes on VTA DA cells were observed after ghrelin administration (100  $\mu\text{g}$  ghrelin in saline or saline alone;  $n = 5$  per group) to *Ghsr*<sup>-/-</sup> animals ( $10.64 \pm 0.62$  versus  $9.89 \pm 0.67$  synapses/100  $\mu\text{m}$  perikaryal membrane;  $P > 0.05$ ; Figure 3).

Quantification of double label-stained VTA sections revealed that ghrelin treatment significantly increased the number of putative excitatory synaptic appositions ( $14.89 \pm 1.87$  versus  $7.35 \pm 0.56$  vGlut appositions/100  $\mu\text{m}$  TH cell;  $t_{17} = 2.66$ ,  $P < 0.05$ ; Figure 4, A and B) and reduced the number of putative inhibitory appositions onto TH-immunoreactive perikarya compared with saline-treated mice ( $6.31 \pm 0.73$  versus  $13.03 \pm 0.73$  GAD-67-immunoreactive appositions/100  $\mu\text{m}$  TH cell;  $t_{13} = -6.21$ ,  $P < 0.05$ ; Figure 4, A and B). A second series of experiments was conducted to determine whether these ghrelin-induced synaptic changes could be detected using electrophysiology. In these studies, we compared the

frequency of miniature excitatory and inhibitory postsynaptic currents (mEPSCs and mIPSCs, respectively) in DA cells from slices of VTA harvested from mice treated with saline or ghrelin (30  $\mu\text{g}$  i.p.) 2 hours before sacrifice. Our results showed that, in correla-

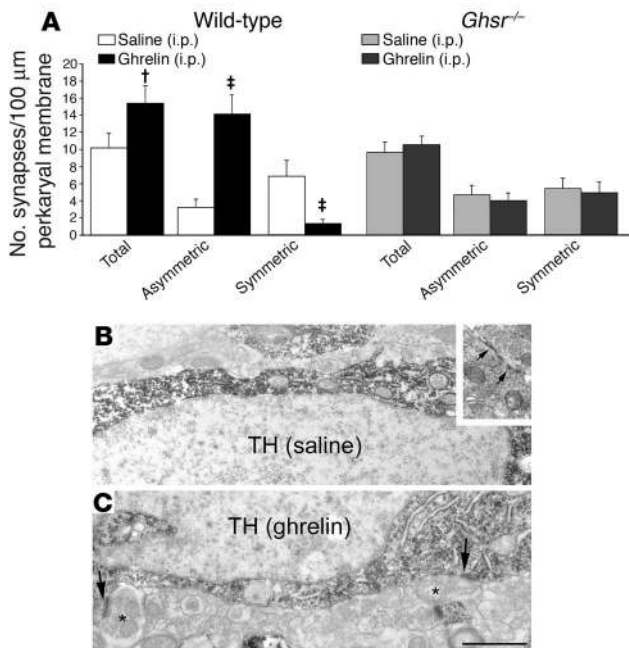


**Figure 3** Synaptic remodeling induced by peripheral ghrelin in VTA DA cells. (A) Ghrelin increased the number of synapses on VTA DA cells of wild-type mice ( $n = 5$ ). Both total and asymmetric synaptic contacts were elevated, while the number of symmetric synapses was decreased. No synaptic changes were observed after peripheral ghrelin injection in *Ghnr*<sup>-/-</sup> mice ( $n = 5$ ). <sup>†</sup> $P < 0.05$ , <sup>‡</sup> $P < 0.01$  versus respective saline-treated controls. (B and C) Electron micrographs showing typical TH-immunoreactive perikarya of the VTA from saline- (B) and ghrelin-treated (C) wild-type mice. Arrows in inset of B indicate a symmetric synapse. Arrows in C indicate asymmetric synaptic contacts. Asterisks indicate unlabeled axon terminals. Scale bar: 1 μm.

tion with the synaptic remodeling, ghrelin treatment significantly increased the frequency of mEPSCs compared with saline treatment ( $77.86 \pm 10.48$  versus  $40.90 \pm 6.63$ ;  $t_{30} = 2.98$ ,  $P < 0.05$ ; Figure 4C). In contrast, the frequency of mIPSCs was significantly decreased in DA cells from ghrelin-treated mice compared with that of saline-treated mice ( $67.55 \pm 10.01$  versus  $107.72 \pm 12.78$ ;  $t_{28} = -2.47$ ,  $P < 0.05$ ; Figure 4D). These data revealed that ghrelin's effects on VTA DA neurons also include induction of synaptic rearrangements in a GHSR-dependent manner in which excitatory synapses dominate the perikarya of these neurons.

*Ghrelin increases DA turnover in the ventral striatum of rats and mice.* To determine whether ghrelin can activate the mesolimbic DA system in vivo, we measured DA turnover in the ventral striatum, a main target site of dopaminergic neuronal projections from the VTA, following either peripheral ghrelin injections (1 mg/kg) or saline injections. Injection of ghrelin in rats i.p. resulted in increased DA turnover in the nucleus accumbens compared with saline-injected controls (dihydroxyphenylacetic acid/DA [DOPAC/DA] ratio, saline,  $0.110 \pm 0.0003$ ; ghrelin,  $0.132 \pm 0.0055$ ;  $t_7 = -3.034$ ,  $P < 0.05$ ; Figure 5A). In a second study, ghrelin-knockout mice were injected with saline or 1 of 2 doses of ghrelin (10 or 30 μg), and their ventral striatum was excised and processed to determine DA turnover. A between-groups ANOVA conducted on these data showed that ghrelin significantly increased DA turnover in the ventral striatum

of ghrelin-knockout mice and did so in a dose-dependent manner (DOPAC/DA ratio, saline,  $0.23 \pm 0.09$ ; 10 μg ghrelin,  $0.456 \pm 0.06$ ; 30 μg ghrelin,  $0.556 \pm 0.05$ ;  $F_{4,19} = 15.49$ ,  $P < 0.05$ ; Figure 5B). On the other hand, peripheral ghrelin administration (100 μg) did not alter DA turnover compared with the effects of saline injections (Figure 5B) in *Ghnr*<sup>-/-</sup> animals.

*Ghrelin infusions into the VTA increase feeding in rats.* The presence of GHSR in the VTA and the ability of ghrelin to bind to this region and alter the activity of DA cells led us to next determine whether ghrelin acts at this site to modulate feeding. Similar to previously reported findings (25), our results confirmed that a single infusion of ghrelin (0.5 μg in 0.5 μl saline) directly into the VTA of awake rats strongly increased food intake during the 2 hours following treatment, which was significantly different from the food intake of saline-treated controls (ghrelin,  $6.16 \pm 0.55$  g; saline,  $1.90 \pm 0.55$  g;  $F_{2,14} = 41.07$ ;  $P < 0.05$ ). In contrast, rats – in which the cannula were misplaced and missed the VTA, as verified by post-hoc histologic examination – did not show increased food intake in response to ghrelin (ghrelin outside the VTA,  $2.17 \pm 0.26$  g;  $P > 0.05$ ; Figure 5C). Thus, if circulating ghrelin reaches the VTA, it is a reasonable suggestion that this orexigenic gut hormone could affect feeding behavior by acting directly in the VTA.

*Peripheral ghrelin-induced feeding responses in rats are attenuated by intra-VTA infusions of a GHSR antagonist.* To test whether circulating ghrelin levels act on the VTA to increase food intake, we assessed the effect of a GHSR antagonist on peripheral ghrelin-induced food intake. The recently developed compound BIM28163 blocks GHSR activation in vitro (26). To study the effect of this GHSR antagonist within the VTA, animals were equipped with cannulae placed just dorsal to the VTA. After an acclimation period, animals were infused with BIM28163 into the VTA (0.5 μg in 0.5 μl saline) and administered peripheral ghrelin (5 μg in 0.1 ml saline) 1 hour later. This dose was chosen because it has been previously shown to increase food intake and elevate plasma ghrelin concentrations to the same degree as a 24-hour fast in rats (27). In the absence of pretreatment of the VTA with BIM28163, ghrelin induced a significant increase in food intake compared with control animals (saline/ghrelin,  $1.91 \pm 0.15$  g; saline/saline,  $1.1 \pm 0.25$  g; BIM28163/saline,  $0.61 \pm 0.19$  g;  $F_{3,33} = 24.40$ ,  $P < 0.05$ ; Figure 5D). Ghrelin treatment, however, failed to increase food intake in rats pretreated with BIM28163 into the VTA (BIM28163/ghrelin,  $0.67 \pm 0.18$  g; Figure 5D). Food intake was not affected by BIM28163 when the infusion of this drug into the VTA was followed by i.p. saline injections, indicating that the antagonist alone has no effect on feeding in satiated animals. These results strongly suggest that exogenous ghrelin from the circulation can reach the VTA in physiologically relevant amounts to elicit a feeding response via activation of the mesolimbic dopaminergic system.

*VTA administration of BIM28163 blunts rebound feeding after fasting in mice.* In order to establish whether GHSRs in the VTA play a role in feeding responses under physiologic conditions, we analyzed interference with GHSR signaling during a fast. Mice were equipped with cannulae aimed at the VTA and connected to osmotic minipumps. Mice were infused chronically with either saline or BIM12863 (3.3 μg/d) at a rate of 0.25 μl/h. This dose was chosen because an acute intra-VTA infusion of a similar dose blocked peripheral ghrelin-induced food intake in rats (see above). Food intake was recorded daily for 6 days following the insertion of the cannula and prior to the 24-hour fast. During this period, animals that were infused with BIM28163 ate, on average, signifi-

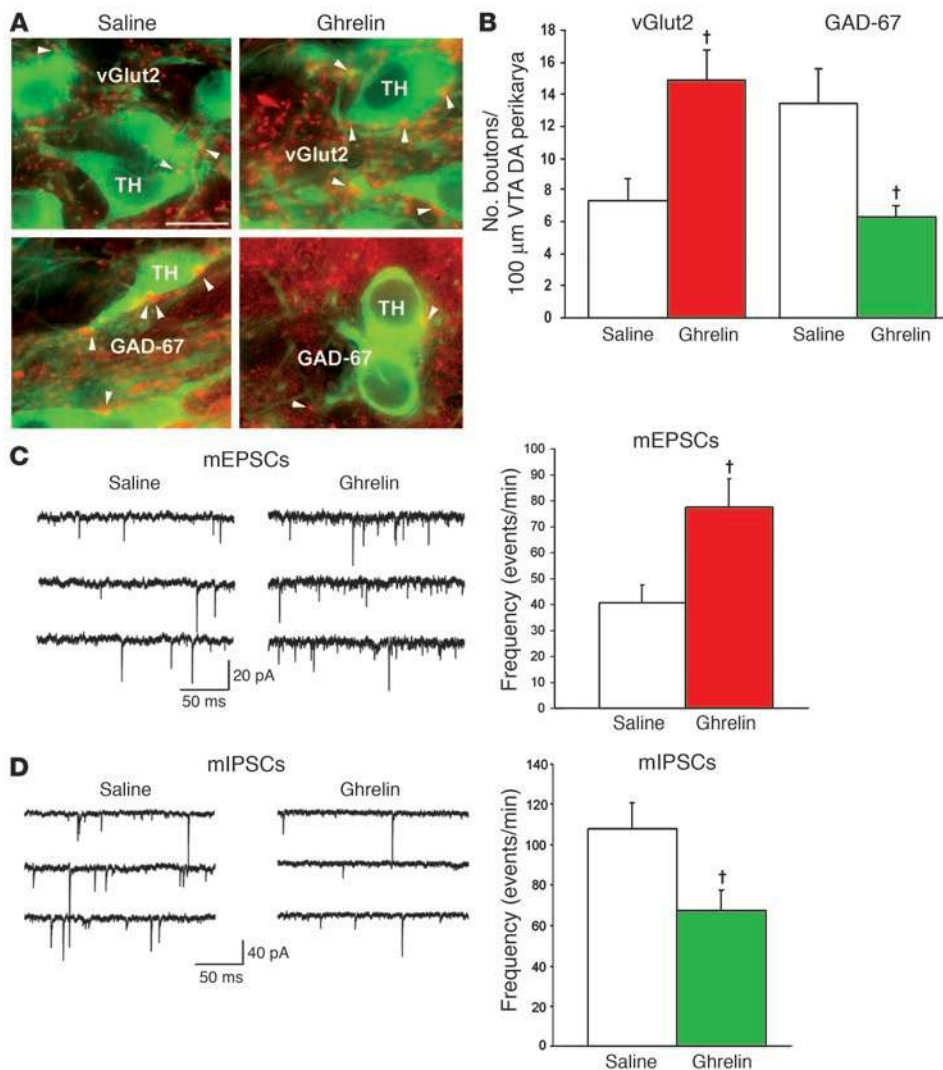


**Figure 4** Ghrelin alters inhibitory and excitatory inputs of VTA DA cells. **(A and B)** Appositions between vGlut2-immunoreactive (red) and TH-immunopositive (green) VTA perikarya were significantly greater in ghrelin-treated animals compared with saline-treated controls. In contrast, appositions between GAD-67-immunolabeled boutons and TH-immunoreactive VTA perikarya were significantly lower in ghrelin-treated animals compared with saline-treated controls. Scale bars: 10 μm. **(C)** Corresponding to the observed changes in the number of synapses by light and electron microscopy, ghrelin treatment induced a significant elevation in the frequency of mEPSCs compared with saline controls. **(D)** Conversely, ghrelin administration triggered a significant decrease in the frequency of mIPSCs that was also in line with the light and electron microscopy results. <sup>†</sup>*P* < 0.05 versus respective saline-treated controls.

cantly less food per day than did control mice (saline, 4.47 ± 0.21 g; BIM28163, 3.36 ± 0.25 g; *t*<sub>7</sub> = -3.46, *P* < 0.05). On the sixth day after surgery, mice were fasted overnight, and their feeding responses were recorded 1, 2, and 6 hours after refeeding. As shown in Figure 5E, mice infused with BIM12863 into the VTA showed significantly attenuated feeding responses 6 hours after the food was returned to their cages (saline, 1.79 ± 0.18 g; BIM28163, 0.91 ± 0.11 g; *F*<sub>1,7</sub> = 9.21, *P* < 0.05). This effect was statistically significant only during the first hour after the food was presented (saline, 0.93 ± 0.04 g; BIM28163, 0.30 ± 0.12 g; *t*<sub>7</sub> = -5.50, *P* < 0.05; Figure 5F), suggesting that mice infused with ghrelin antagonists into the VTA have decreased appetite in response to fasting.

*Ghrelin-knockout and GHSR-knockout mice show attenuated feeding responses to repeated fasting schedules.* There is a substantial amount of evidence supporting the notion that cues predicting access to rewards such as food are as effective in activating the mesolimbic reward system as the rewards themselves (15, 16, 28). Temporal cues that predict food availability are of particular interest because they seem to activate reward circuits and to generate behavioral food-anticipatory responses like increased locomotor activity that could be associated with increased activity of the mesolimbic dopaminergic system (29, 30). Because of this, and to further

examine whether ghrelin has any physiologic effect on food intake, we analyzed ghrelin-knockout and GHSR-knockout animals on a restricted feeding schedule (Figure 5, G and H). In this paradigm, animals that ingested similar amounts of food before the experiment began were fasted overnight, and food was made available for 6 hours. Feeding responses over the 6 hours in which animals had access to food following the first night of fasting were comparable between wild-type and ghrelin-knockout mice as well as wild-type and GHSR-knockout mice. However, neither ghrelin-knockout (*F*<sub>6,36</sub> = 2.36, *P* < 0.05) nor GHSR-knockout mice (*F*<sub>6,60</sub> = 2.89, *P* < 0.05) increased their food intake at the rate observed in wild-type mice in response to the repeated fast (Figure 5, G and H). This difference was evident on the fourth and fifth days of the restricted feeding schedule in ghrelin-knockout and GHSR-knockout mice, respectively (*P* < 0.05). Thus, the absence of ghrelin signaling appears to result in some deficits in preventative or catch-up hyperphagia, suggesting that ghrelin is important for the full display of feeding behavior in anticipation of a meal.

**Discussion**

The present results revealed that ghrelin targets cells within the VTA to modulate the activity of DA neurons and behaviors associated

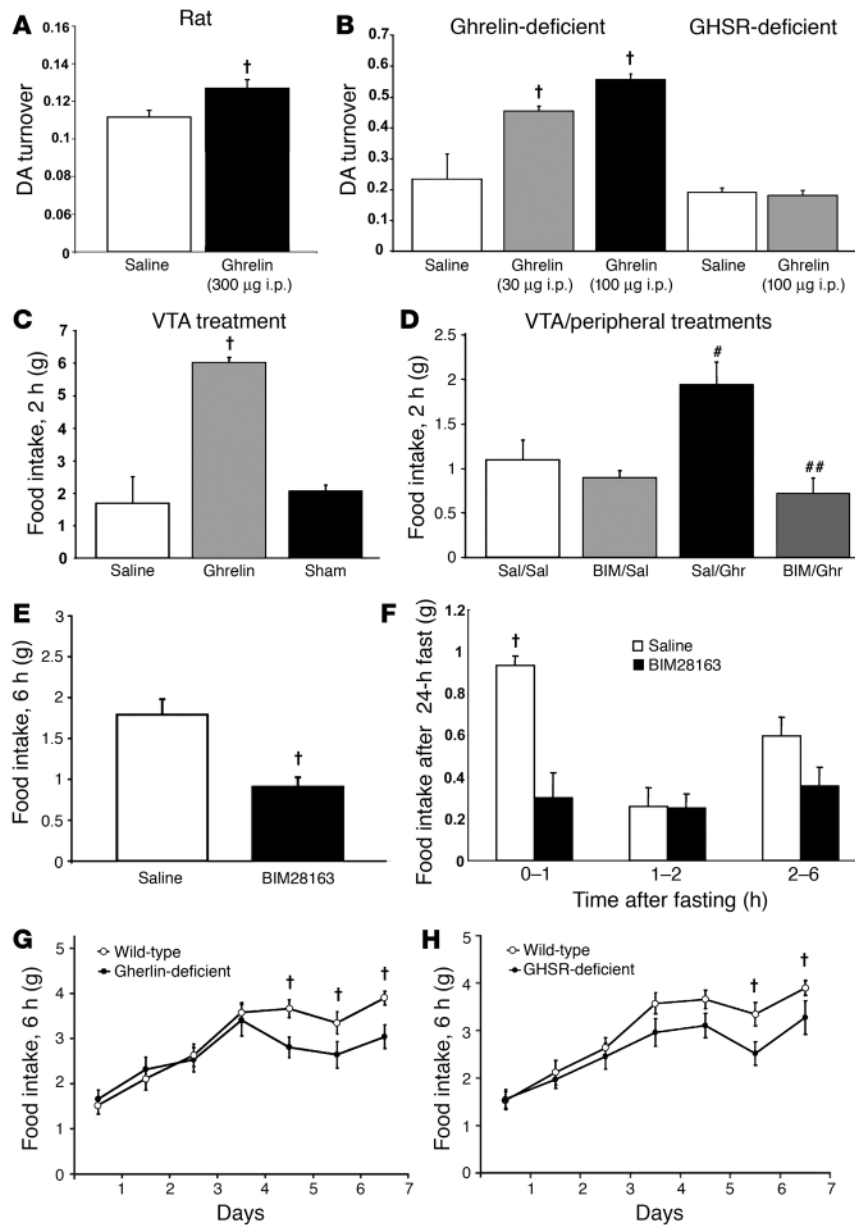


**Figure 5**

Ghrelin alters dopamine turnover and feeding via the VTA. (A) Peripheral ghrelin treatment (1 mg/kg) was effective in increasing DA turnover in the nucleus accumbens of rats ( $n = 12$ ). (B) Ghrelin treatment (30 or 100 µg) of ghrelin-deficient mice increased DA turnover in the ventral striatum in a dose-dependent manner compared with saline-treated mice. Conversely, ghrelin induced no alterations in DA turnover of the nucleus accumbens in *Ghsr*<sup>-/-</sup> mice ( $n = 5$  per treatment). (C) VTA ghrelin infusions (0.5 µg in 0.5 µl saline) significantly increased food intake in rats compared with saline infusions or with infusions at sites adjacent to, but not in, the VTA (Sham). (D) Ghrelin (5 µg in 0.1 ml saline) injected i.p. increased food intake compared with saline-injected rats, an effect blocked by BIM28163 infusion (0.5 ng in 0.5 µl saline) directly into the VTA. (E and F) Rebound feeding 6 hours after fasting was significantly attenuated in mice treated with BIM12863 (1 nM/d) infused into the VTA at 0.25 µl/h (E). This effect was statistically significant only during the first hour after food was reintroduced (F). (G and H) Six-hour food intake in ghrelin- (G) and GHSR-deficient (H) mice under a restricted feeding schedule. Both ghrelin- and GHSR-deficient mice showed attenuated feeding responses after repeated overnight fasts. † $P < 0.05$  versus respective controls. \* $P < 0.05$  versus saline/saline and BIM28163/saline treatment groups; \*\* $P < 0.05$  versus saline/ghrelin treatment group.

with the mesolimbic reward circuit. We found that ghrelin bound to cells in the VTA of rats, where GHSRs were expressed in both dopaminergic and nondopaminergic cells. Overall, these findings are in agreement with the work of Guan et al. (11) showing the presence of mRNA for the GHSR in this region. Furthermore, a recent study (12) also colocalized *Ghsr* mRNA with VTA DA neurons in an abundance similar to what we report here regarding protein expression. We observed that ghrelin acutely elevated the frequency of action potentials of VTA DA neurons, which was dependent on GHSR and excitatory synaptic input. Ghrelin injections in live animals also caused reorganization of synaptic inputs of VTA DA cells, in which asymmetric, putative excitatory inputs dominated the perikarya of these catecholaminergic cells. The activation of VTA DA neurons by ghrelin was also found to induce increased DA turnover in the nucleus accumbens, an effect that was dependent on GHSR.

It is reasonable to suggest that the overall activation of DA cells by ghrelin arises not only from direct electrophysiologic effects,

but also from ghrelin's ability to rapidly rearrange the synaptic input of DA neurons in a manner that would increase the probability of activation of these cells by other inputs as well. This effect of ghrelin on synapses is consistent with previous findings in the hypothalamus (23) and hippocampus (31). Our data also promote the notion that the VTA is a highly plastic area of the brain and that this plasticity is an important component for motivated behaviors in response to orexigenic signals (24, 32–34). Further investigation will be required to determine the intracellular signaling modality that brings about these rapid changes as well as the parent cell of origin of the altered inputs in wiring. Another fundamental question regarding these synaptic changes is whether it requires signaling of ghrelin on the pre- and/or postsynaptic sites. Based on the association between ghrelin-induced synaptic plasticity and the dependence of ghrelin's electrophysiologic action in the VTA (present results) and hypothalamus (5) on presynaptic mechanisms, it is tempting to speculate that these morphologic



changes represent activity-dependent synaptic plasticities. In support of this notion, those neurons in the hypothalamus that produce neuropeptide Y and directly respond to ghrelin without the need of presynaptic mediation (5) showed no synaptic changes on their perikarya (23) in the same ghrelin paradigm that showed synaptic changes on VTA DA (present results) and hypothalamic pro-opiomelanocortin neurons (23).

We found that, similar to another recent experiment (25), feeding responses were dramatically increased when ghrelin was infused into the VTA of rats with free access to food. Our observations of increased food intake 2 hours after delivery of ghrelin into rat VTA are comparable to those seen in rats that are fasted overnight (for example, see ref. 35). That ghrelin acts in the VTA was further confirmed when ghrelin failed to elicit feeding responses when the cannulae hit adjacent caudal and/or dorsal regions. In addition, we also showed that feeding induced by peripheral injections of ghrelin was attenuated in animals that were given intra-VTA infusions of a GHSR antagonist, which itself had no impact on feeding. Taken together, these results suggest that GHSRs in the VTA, and possibly in the adjacent substantia nigra, modulate feeding behavior in response to fluctuating peripheral levels of endogenous ghrelin. As the present experiments involved the exposure of neurons to various doses of exogenous, synthetic ghrelin, the physiologic significance of these studies require further confirmation.

While ghrelin induces robust feeding responses when infused into the VTA, it seems unlikely that ghrelin targets the VTA to modulate food intake selectively, because reward circuits are also responsive to a variety of natural and synthetic compounds that promote reward or reward seeking. It appears more likely that ghrelin, like caloric restriction, increases the sensitivity of the VTA to the effect of reward-seeking or reward-inducing stimuli in general, whether it is food, drugs of abuse, or the lack thereof (36). DA cells in the VTA and their projections have been implicated in food and drug reward-seeking behaviors in animals and humans (37–41), and the presence of DA is necessary to maintain appetitive responses toward food (42, 43). In addition, DA is also released in situations where rewards can be predicted using environmental cues (15). Using circadian time as a cue predicting food availability as it occurs in scheduled feeding paradigms, ghrelin- and GHSR-knockout animals exhibited blunted feeding responses, even though they had no impairment in normal feeding or rebound feeding after an acute 24-hour fast. In light of the facts that repeated fasting is associated with increased activity both in cells in hypothalamic centers regulating energy balance and in cells in target regions of the VTA and that ghrelin stimulates DA release in these same regions, it is possible that the lack of ghrelin or GHSRs leads to impairments in mechanisms related to food anticipation (29, 30, 44). On the other hand, rebound feeding after an acute fast was not altered in adult GHSR-knockout mice, but was decreased in normal adult mice infused with a GHSR antagonist into the VTA. It may be that these results in the genetically altered mice were due to developmental alterations caused by the lack of ghrelin signaling, which in turn could mask acute effects of ghrelin in the adult. Interestingly, rebound feeding in mice infused with ghrelin antagonists into the VTA was reduced primarily during the first hour after the food was returned. This finding, together with the observation that GHSR- and ghrelin-knockout mice are less susceptible to palatable high-fat diets (45, 46), support the idea that a lack of ghrelin signaling in the VTA leads primarily to deficits in appetitive responses to readily available food, implicat-

ing GHSRs in the VTA as physiologic mediators of appetite. Furthermore, high circulating levels of ghrelin are associated with the intense food cravings of patients with Prader-Willi syndrome, and the weight loss and diminished appetite observed following gastric bypass surgery correlates with decreased blood ghrelin levels (47–49). Whether the antagonism of GHSRs may offer not only an alternative to counteract cravings for calorie-rich food but also a novel approach to pharmacologically fight drug addiction and/or relapse is a clinically relevant and important avenue to pursue.

Activation of mesolimbic dopaminergic neurons by stimuli with rewarding properties is often linked with increased DA turnover in the regions targeted by these neurons. In the present study, we found that peripheral ghrelin treatment increased DA turnover in the ventral striatal regions of both mice and rats, even when the animals were not given food after the injection. This again suggests that peripheral ghrelin can stimulate dopaminergic cells in the VTA to produce a net increase in DA turnover, an event directly related to reward mechanisms (14). Shuto et al. have previously shown that rats made to endogenously overexpress an antisense to the GHSR under the activity of TH (a rate-limiting enzyme for DA) promoter, thereby knocking down GHSR expression, eat and weigh less than those that do not produce the antisense (50). In light of the effects of ghrelin and ghrelin antagonists on the VTA, it is conceivable that the reported metabolic effects of those transgenic rats are mediated primarily by DA cells in the VTA and adjacent substantia nigra, where GHSR/TH colocalization is more prominent (12).

In conclusion, the present results show that the metabolic gut hormone ghrelin can directly affect functional correlates of the mesolimbic reward circuitry to modulate food intake and indicate that through the VTA, ghrelin may be an important factor in the etiology of pathologies associated with food as well as drugs of abuse.

## Methods

### Animals

Male Sprague-Dawley rats (240–260 g) and C57BL/6 mice were purchased from Charles River Laboratories and The Jackson Laboratory, respectively. Animals were kept under standard laboratory conditions, with tap water and regular rat chow available ad libitum, in a 12-hour light/12-hour dark cycle. Animals were group housed (3 animals per cage) until surgical manipulations were conducted.

Ghrelin- and GHSR-knockout (on a C57BL/6 and C57BL/J6 background) mice were obtained from Regeneron Pharmaceuticals and bred in our facilities. The characterization of both genetically engineered mice has been described previously (51).

All procedures in this study were conducted under NIH guidelines for the use of animals in research and approved by the Yale University Animal Care Committee.

### Biotinylated ghrelin binding

To assess the ability of ghrelin to bind to cells in the VTA and nucleus accumbens, 100- $\mu$ m sections containing these regions were processed for binding studies as described previously (5). In short, saline-perfused rat brains ( $n = 4$ ) were removed, sectioned, and immediately reacted with biotinylated ghrelin (1 M; Phoenix Pharmaceuticals Inc.) alone or in combination with an equal amount of unlabeled (cold) ghrelin (1 M; Phoenix Pharmaceuticals Inc.) for 20 minutes at 4°C. Subsequently, sections were fixed with 4% paraformaldehyde, reacted with avidin-Texas red, and analyzed using a Zeiss microscope equipped with filters selective to various wavelength of fluorescent light.



### Single-label immunoreactivity for GHSR in the mesolimbic reward circuitry

Male rats ( $n = 4$ ) were anesthetized and transcardially perfused with 0.9% saline followed by fixative (4% paraformaldehyde, 15% picric acid, and 0.08% glutaraldehyde in 0.1 M phosphate buffer [PB]). Brains were collected, postfixed overnight and sectioned. Sections of 50  $\mu\text{m}$  across the rostrocaudal extent of the forebrain and midbrain were then processed for immunocytochemistry using rabbit antisera raised against the Cys (aa residues 330–366) portion of the human GHSR sequence (Phoenix Pharmaceuticals Inc.). Control sections were incubated in antibody preabsorbed with the human GHSR protein (20 mg/ml) or without primary antiserum. The protocol was as follows: Sections were washed several times and reacted with 1%  $\text{H}_2\text{O}_2$  in 0.1 M PB solution for 30 minutes. Following several washes, sections were incubated in a 10% sucrose solution for 2 hours for cryoprotection, snap-frozen in liquid nitrogen, and thawed. After washing several times, slices were incubated in blocking serum (2% normal horse serum in 0.1 M PB) for 1 hour and incubated in primary antibody (diluted 1:1,000 in blocking solution) for 72 hours at 4 °C. After several washes with PB, sections were incubated in biotinylated donkey anti-rabbit (diluted 1:250; The Jackson Laboratory) for 2 hours at room temperature, washed, and incubated in avidin-biotin complex (VECTASTAIN Elite ABC Kit; Vector Laboratories) for 2 hours at room temperature. The tissue-bound peroxidase was visualized by a nickel-diaminobenzidine reaction (5 mg DAB, 6.5 mg ammonium chloride, 780  $\mu\text{l}$  nickel ammonium sulfate, 16 ml PB, and 425  $\mu\text{l}$  0.03% hydrogen peroxide) at room temperature for 4 minutes, resulting in a black reaction product. Following washing, sections were mounted and coverslipped in Depex mounting medium (Electron Microscopy Sciences). The same procedure was conducted on brain sections from wild-type and GHSR-knockout mice; no staining was observed in the latter (Figure 1) or in the negative controls.

$\beta$ -Gal, the product of the *LacZ* gene in the place of *Ghsr* gene, was visualized as described by Wortley et al. (51).

### Double immunofluorescence for GHSR and TH

Tissue sections from the rats used in the single-label GHSR immunocytochemistry study were stained for GHSR in a manner similar to that described above, except that the primary antibody solution also contained mouse anti-TH (a well-known marker for DA-synthesizing cells, diluted 1:1,000; Chemicon International). Sections were then washed and incubated for 2 hours at room temperature in a solution containing donkey anti-rabbit Alexa Fluor 594 IgG (diluted 1:200, red immunofluorescence; Invitrogen) to visualize GHSR plus donkey anti-mouse Alexa Fluor 488 IgG (green fluorochrome; Invitrogen) to visualize TH. Fluorescence-labeled sections were washed and mounted in Vectashield medium and coverslipped for immunofluorescence examination.

### Double immunofluorescence for vGlut or GAD-67 and TH

Tissue sections containing the VTA of saline- and ghrelin-treated (100  $\mu\text{g}$ ) mice were processed for either vGlut2 and TH or GAD-67 and TH immunofluorescence using a protocol similar to that described above. In these studies, sections were incubated overnight in 1 of 2 primary antibody cocktails. The first contained a combination of guinea pig anti-vGlut2 antisera and mouse anti-TH antibodies (diluted 1:2,000; both from Chemicon International). The second set of sections were incubated in a cocktail containing rabbit anti-GAD-67 antisera (diluted 1:1,000; Chemicon International) and mouse anti-TH antibodies. The following day, sections were incubated in donkey anti-mouse Alexa Fluor 488 IgG (green fluorochrome; Invitrogen) to visualize TH and goat anti-guinea pig or -rabbit Alexa Fluor 594 IgG (diluted 1:200, red immunofluorescence; Invitrogen) to visualize vGlut2 or GAD-67. Once coverslipped, sections were analyzed

at high power using a Zeiss Axiophot microscope with capabilities of visualizing and detecting fluorescent light to quantify and compare vGlut2- and GAD-67-containing boutons making putative contact with TH cells. The mean number of vGlut2 and GAD-67 boutons in close contact with TH perikarya were compared between saline- and ghrelin-treated animals using unpaired 2-tailed Student's *t* tests.

### Patch clamp recordings from VTA DA neurons

Brain slices (300  $\mu\text{m}$ ) containing the VTA from 2- to 3-week-old male and female mice ( $n = 9$ ) and rats ( $n = 5$ ) were cut on a vibratome. Briefly, animals were anesthetized with Nembutal (80 mg/kg) and then decapitated. The brains were rapidly removed and immersed in cold (4 °C) oxygenated bath solution (150 mM NaCl; 2.5 mM KCl; 2 mM  $\text{CaCl}_2$ ; 2 mM  $\text{MgCl}_2$ ; 10 mM HEPES; and 10 mM glucose, pH 7.3, with NaOH). After being trimmed to contain only the VTA, slices were transferred to a recording chamber, where they were constantly perfused with bath solution at 2 ml/min. DA neurons in the VTA were identified by presence of a large Ih current (>100 pA) evoked by hyperpolarizing voltage steps from -50 to -120 mV for 2 seconds (22). This approach identifies VTA dopaminergic cells with greater than 90% accuracy (22). In brain slices, a whole-cell current clamp was used to observe spontaneous action potentials. Slices were maintained at 33 °C and perfused continuously with artificial cerebrospinal fluid (ACSF) (bubbled with 5%  $\text{CO}_2$  and 95%  $\text{O}_2$ ) containing 124 mM NaCl; 3 mM KCl; 2 mM  $\text{CaCl}_2$ ; 2 mM  $\text{MgCl}_2$ ; 1.23 mM  $\text{NaH}_2\text{PO}_4$ ; 26 mM  $\text{NaHCO}_3$ ; and 10 mM glucose, pH 7.4, with NaOH. Ghrelin was applied to the recording chamber via bath application. The pipette solution contained 140 mM gluconic acid; 2 mM  $\text{CaCl}_2$ ; 2 mM  $\text{MgCl}_2$ ; 1 mM EGTA; 10 mM HEPES; 4 mM Mg-ATP; and 0.5 mM  $\text{Na}_2$ -GTP, pH 7.3, with KOH. To further verify the effect of ghrelin on the frequency of action potentials in DA neurons in the VTA, we used GHSR-knockout mice as described above.

To further explore the mechanism of the ghrelin-mediated effect on action potentials in DA neurons, we analyzed the effect of ghrelin on action potential frequency either in the presence of ionotropic glutamate receptor antagonists CNQX (10  $\mu\text{M}$ ) and AP5 (50  $\mu\text{M}$ ) in all solutions or in the presence of bicuculline (30  $\mu\text{M}$ ; to diminish GABA effects) in all solutions.

All data were sampled at 3–10 kHz and filtered at 1–3 kHz with a Macintosh computer using AxoGraph version 4.9 (Axon Instruments). Electrophysiologic data were analyzed with AxoGraph version 4.9 and plotted with IGOR Pro software (version 5.04; WaveMetrics).

### Analysis of mEPSCs and mIPSCs

Mice (C57BL/J6;  $n = 10$ ) aged 21–30 days were injected with ghrelin (30  $\mu\text{g}$  in 0.3 ml) or vehicle i.p. Two hours later, animals were sacrificed under nembutal anesthesia, and their brains were collected as described in our previous electrophysiologic studies (52). For the recording of mEPSCs and IPSCs, VTA DA cells were patched with pipettes with a tip resistance of 4–6 M $\Omega$  and partially compensated by the amplifier. The pipette was filled with a solution containing 145 mM KMeSO (mEPSCs) or KCL (mIPSCs); 2 mM  $\text{MgCl}_2$ ; 10 mM HEPES; 2 mM Mg-ATP; 0.3 mM  $\text{Na}_2$ -GTP; and KOH to adjust the pH to 7.3. mEPSC recordings were taken in the presence of tetrodotoxin (TTX) and bicucullin, whereas mIPSCs were monitored in the presence of TTX, AP5, and CNQX. The frequency and amplitude of mEPSCs and mIPSCs were determined as described previously (52). Differences in the frequency of mEPSCs and mIPSCs of DA cells from ghrelin- and saline-treated animals were compared using unpaired 2-tailed Student's *t* tests with the critical level set at  $\alpha = 0.05$ .

### Synaptic analysis of TH-immunolabeled VTA neurons

Tissue blocks containing the VTA were dissected from each brain ( $n = 5$  per group). Vibratome sections (50  $\mu\text{m}$  thick) were cut and washed in





0.1 M PB. To eliminate unbound aldehydes, sections were incubated in 1% sodium borohydride for 15 minutes and then rinsed in PB. Subsequently, sections were incubated in mouse anti-TH antisera for 24 hours at room temperature followed by incubation in biotinylated horse anti-mouse Ig (diluted 1:250; Vector Laboratories) for 2 hours at room temperature. Sections were then incubated in avidin-biotin complex (2 hours at room temperature; VECTASTAIN Elite ABC Kit; Vector Laboratories), and the tissue-bound peroxidase was visualized by a diaminobenzidine reaction. After immunostaining, the sections were osmicated (15 minutes in 1% osmium tetroxide in PB) and dehydrated in increasing ethanol concentrations. During the dehydration, 1% uranyl acetate was added to the 70% ethanol to enhance ultrastructural membrane contrast. Dehydration was followed by flat-embedding in Araldite. Ultrathin sections were cut on a Leica ultramicrotome, collected on Formvar-coated single-slot grids, and analyzed with a Tecnai 12 BioTWIN (FEI Co.) electron microscope.

The quantitative and qualitative analysis of synapse number was performed in a blinded fashion. To obtain a complementary measure of axosomatic synaptic number, unbiased for possible changes in synaptic size, the dissector technique was used. On consecutive 90-nm-thick sections we determined the average projected height of the synapses and used about 30% of this value as the distance between the dissectors. On the basis of this calculation, the number of axosomatic synapses was counted in 2 consecutive serial sections about 270 nm apart (termed *reference* and *look-up* sections) of 10 TH-immunolabeled perikarya profiles in each animal. Synapse characterization was performed at a magnification of 20,000. Symmetric and asymmetric synapses were counted on all selected neurons only if the pre- and/or postsynaptic membrane specializations were seen and synaptic vesicles were present in the presynaptic bouton. Synapses with neither clearly symmetric nor asymmetric membrane specializations were excluded from the assessment. The plasma membranes of selected cells were outlined on photomicrographs, and their length was measured with the help of a cartographic wheel. Plasma membrane length values measured in the individual animals were added, and the total length was corrected to the magnification applied. Synaptic densities were evaluated according to the formula  $NV = Q_-/V_{dis}$ , where  $NV$  represents number per volume and  $Q_-$  represents the number of synapses present in the reference section that disappeared in the look-up section and  $V_{dis}$  is the dissector volume (volume of reference), the area of the perikarya profile multiplied by the distance between the upper faces of the reference and look-up sections (i.e., the data are expressed as numbers of synaptic contacts per unit volume of perikaryon). Section thickness was determined using the Small's minimal fold method (53). The synaptic counts were expressed as numbers of synapses on a 100- $\mu$ m membrane length unit. Unpaired 2-tailed Student's  $t$  tests were used to determine significance of differences between groups.

### **Nucleus accumbens DA levels**

In order to test for the potential alterations in DA output of the VTA, we analyzed DA turnover in the nucleus accumbens, a major target area of VTA DA neurons. In the first experiment, rats ( $n = 12$ ) were injected i.p. with saline or ghrelin (1 mg/kg) daily for 3 days and sacrificed 2 hours following the last injection. At the time of sacrifice, the ventral striatum was rapidly dissected on a chilled glass plate and frozen at  $-70^\circ\text{C}$ . In the second study, ghrelin- and GHSR-knockout mice as well as wild-type controls were assigned to groups receiving 1 of 3 different ghrelin doses (10, 30, or 100  $\mu$ g) or saline and sacrificed 60 minutes later. The ventral striatum was dissected as described above, and tissue samples were rapidly frozen and stored until analyses were conducted. The samples were subsequently thawed in 0.4 ml of chilled 0.1 M perchloric acid and sonicated. Aliquots were taken for protein quantification using a spectrophotometric assay. Other aliquots were centrifuged, and DA levels were measured in super-

natants by HPLC with electrochemical detection. The DOPAC concentration (expressed as ng/mg protein) was divided by the DA concentration to determine DA turnover. Neither rats nor mice had access to food following the ghrelin injection or before being sacrificed. Differences in DA turnover between ghrelin- and saline-treated rats were analyzed using an unpaired 2-tailed Student's  $t$  test, whereas 1-way, between-groups ANOVA was conducted to evaluate mean differences in saline- and ghrelin-treated mice.

### **Intracranial cannula implantation**

*Intracranial cannulae aimed at the VTA in rats.* Rats were anesthetized with an i.p. injection of a ketamine/xylazine cocktail (7.5 mg ketamine, 0.3 mg xylazine, and 0.19 mg acepromazine per 100 g body weight) and placed in the stereotaxic apparatus (Kopf Instruments). The scalp was shaved slightly posterior to the eyes up to the base of the skull. A sagittal incision approximately 2.5 cm in length was made, the skin was retracted, and the skull was exposed and cleaned. Unilateral cannulae were aimed at the VTA (coordinates: AP,  $-5.3$ ; L,  $+1.0$ ; VM,  $-7.6$ ) with the incisor bar at the level of the interaural line and the cannula angled 10 degrees toward the midline of the brain. Cannulae were anchored to the skull with screws and dental cement. The correct placement of cannulae was determined by histologic examination. Brain sections were stained with cresyl violet, and the tips of the cannulae were located. Rats in which the cannulae were found to be misplaced were analyzed as an independent group. The distribution of cannulae placements is shown in Supplemental Figure 1 (supplemental material available online with this article; doi:10.1172/JCI29867DS1). In addition, VTA-cannulated animals ( $n = 2$ ) were deeply anesthetized and infused with 0.5  $\mu$ l Coomassie blue dye. Animals were sacrificed 20 minutes later by either intracardial perfusion or decapitation, and their brains were collected to assess the spread of the infusion. As seen in Supplemental Figure 1, the spread of the infusion was confined to the anatomic location of the VTA.

*Intracranial cannulae aimed at the VTA in mice.* Mice of the C57BL/6 strain were matched by weight and assigned to 1 of 2 groups according to the drug infused (saline or BIM12863), anesthetized with a mixture of oxygen and isoflurane, and mounted onto the stereotaxic apparatus. A sagittal incision approximately 2.5 cm in length was made, the skin was retracted, and the skull was exposed and cleaned. Unilateral cannulae (Plastic One) connected to ALZET Osmotic minipumps (model 1002) were aimed at the VTA (coordinates: AP,  $-2.9$  mm; L,  $+1.0$  mm; VM,  $-4.4$  mm) with the incisor bar at the level of the interaural line and the cannulae angled 10 degrees toward the midline of the brain. The cannulae were secured to the skull with contact glue and dental cement. Once the cement solidified, an incision was made in the intrascapular space to insert the minipump. The incision was then sutured, and the mice were allowed to recover for a period of 48 hours before data collection began. The correct placement of cannulae was determined by histologic examination. Brain sections were stained with cresyl violet, and the tips of the cannulae were located. Mice in which the cannulae were found to be misplaced were not included in the data analyses. A total of 9 mice were considered for the final analyses (saline,  $n = 5$ ; BIM12863,  $n = 4$ ). The distribution of cannulae placements is shown in Supplemental Figure 2.

### **Central ghrelin and GHSR antagonist administration**

*Effects of intra-VTA ghrelin infusions.* Following cannulae implantation, rats ( $n = 15$ ) were allowed to recover as described above. On the experimental day, animals received either saline or ghrelin (0.5 mg in 0.5 ml saline), and food intake was recorded 2 hours later. Animals were then sacrificed, and their brains were obtained to confirm the placement of the cannulae (see Supplemental Figure 1). Mean food intake was compared using 1-way, between-groups ANOVA with Fisher PLSD post-hoc comparisons.



*Effects of intra-VTA infusions of BIM28163 on peripheral ghrelin-induced food intake.* After recovery from surgery, rats ( $n = 15$ ) received infusions of saline or BIM28163 (5  $\mu\text{g}$  in 0.05  $\mu\text{l}$  saline) followed by i.p. injections of saline or ghrelin (5  $\mu\text{g}$  in 0.1 ml saline) 30 minutes later. In this study, all animals received all drug treatments, varying only in the order in which each treatment was administered, using a Latin square design (54). Data were organized to show the average change in food intake following each treatment from the baseline food intake of each animal prior to the drug treatment. The mean change in food intake after each treatment was analyzed using within-groups ANOVA with treatment and injection order as variables followed by individual post-hoc paired 2-tailed Student's  $t$  tests. Animals were sacrificed at the end of the study, and their brains were obtained to confirm the placement of the cannulae. Intracranial infusions of BIM28163 into the VTA did not elicit any observable effects on food intake or on the general health of the animals.

*Effects of intra-VTA chronic infusions of BIM28163 on fasting-induced food intake.* C57BL/J6 mice ( $n = 15$ ; The Jackson Laboratory) were equipped with cannulae aimed at the VTA and connected to an osmotic minipump that delivered either saline or BIM28163 (1 nm/d) at a rate of 0.25  $\mu\text{l}/\text{h}$ . After surgery, food intake and body weights were recorded daily for 6 days. On the sixth day, food was measured and removed from the cage overnight. A pre-weighed amount of food was presented the next morning, and after 1, 2, and 6 hours, the food intake of the mice was measured. Animals were then sacrificed by transcardial perfusion of saline followed by 4% paraformaldehyde, and brains were processed for histologic examination of cannulae placements. Data from only 9 mice (vehicle-infused,  $n = 5$ ; BIM28163-infused,  $n = 4$ ) were considered for analysis given the localization of cannulae. A repeated-measures ANOVA with treatment (saline or BIM28163) as the between-subjects factor and time after refeeding (1, 2, 4, and 6 hours) as the within-group factor was conducted to compare the food intake of these mice after the fast. Post-hoc unpaired 2-tailed Student's  $t$  tests were conducted to evaluate overall differences in rebound feeding after the fast between saline- and BIM28163-infused mice at each individual time point.

**Repeated fast in wild-type and ghrelin- and GHSR-deficient mice**

Mice were individually housed in single cages for 1 week to allow for the stress of separation to subside. Following this period, food was removed from their cages overnight and returned to them the following morning. Mice had access to the food for a period of 6 hours, during which their intake was measured 1, 2, 4, and 6 hours after refeeding. Food was then removed until the following morning at the same time. This process was

repeated for a period of 1 week. In this paradigm, control animals readjusted their feeding patterns to consume most of their ad libitum daily food intake during the 6 hours in which the animals have access to food. Two repeated-measures ANOVAs with genotype being the independent variable and experimental day being the within-group variable were conducted. The first ANOVA was used to analyze the food intake data of wild-type and ghrelin-knockout mice, and the second to compare the same data from GHSR-knockout mice and their wild-type littermates. Post-hoc unpaired 2-tailed Student's  $t$  tests were conducted to evaluate differences in food intake at specific time points.

**Statistics**

Data are expressed as mean  $\pm$  SEM unless otherwise indicated. Statistical differences among groups were determined by unpaired 2-tailed Student's  $t$  tests and between-groups, within-groups, and repeated-measures ANOVA as specified throughout Methods. A level of confidence of  $P < 0.05$  was employed for statistical significance.

**Acknowledgments**

This work was supported by NIH grants DK060711, DK074386, AG022880, and NS041725 to T.L. Horvath; DK070723 to X.-B. Gao; DK069987 and DK056863 to M.H. Tschop; MH014092 and MH057483 to R.H. Roth; and AA15632 to M.R. Picciotto and by a National Science and Engineering Research Council of Canada postdoctoral fellowship to A. Abizaid. We wish to thank Rakesh Data, Michael Culler, Heather Halem, and Jesse Z. Dong from Ipsen Inc. for providing the GHSR antagonist BIM28613. We are also indebted to Kashmira Patel and Gita Thanarajasingman for their comments and technical support.

Received for publication July 26, 2006, and accepted in revised form September 19, 2006.

Address correspondence to: Tamas L. Horvath, Section of Comparative Medicine, Yale University School of Medicine, 375 Congress Avenue, LSOG 117, New Haven, Connecticut 06519, USA. Phone: (203) 785-2525; Fax: (203) 785-7499; E-mail: [tamas.horvath@yale.edu](mailto:tamas.horvath@yale.edu).

Alfonso Abizaid's present address is: Department of Psychology and Institute for Neuroscience, Carleton University, Ottawa, Ontario, Canada.

1. Van der Lely, A.J., Tschop, M., Heiman, M.L., and Ghigo, E. 2004. Biological, physiological, pathophysiological, and pharmacological aspects of ghrelin. *Endocr. Rev.* **25**:426-457.
2. Kojima, M., et al. 1999. Ghrelin is a growth-hormone-releasing acylated peptide from stomach. *Nature.* **402**:656-660.
3. Tschop, M., Smiley, D.L., and Heiman, M.L. 2000. Ghrelin induces adiposity in rodents. *Nature.* **407**:908-913.
4. Nakazato, M., et al. 2001. A role for ghrelin in the central regulation of feeding. *Nature.* **409**:194-198.
5. Cowley, M.A., et al. 2003. The distribution and mechanism of action of ghrelin in the CNS demonstrates a novel hypothalamic circuit regulating energy homeostasis. *Neuron.* **37**:649-661.
6. Toshinai, K., et al. 2003. Ghrelin-induced food intake is mediated via the orexin pathway. *Endocrinology.* **144**:1506-1512.
7. Lawrence, C.B., Snape, A.C., Baudoin, F.M., and Luckman, S.M. 2002. Acute central ghrelin and GH secretagogues induce feeding and activate brain appetite centers. *Endocrinology.* **143**:155-162.
8. Bennett, P.A., et al. 1997. Hypothalamic growth hormone secretagogue-receptor (GHS-R) expression is regulated by growth hormone in the rat. *Endocrinology.* **138**:4552-4557.
9. Howard, A.D., et al. 1996. A receptor in pituitary and hypothalamus that functions in growth hormone release. *Science.* **273**:974-977.
10. Nogueiras, R., et al. 2004. Regulation of growth hormone secretagogue receptor gene expression in the arcuate nuclei of the rat by leptin and ghrelin. *Diabetes.* **53**:2552-2558.
11. Guan, X.M., et al. 1997. Distribution of mRNA encoding the growth hormone secretagogue receptor in brain and peripheral tissues. *Brain Res. Mol. Brain Res.* **48**:23-29.
12. Zigman, J.M., Jones, J.E., Lee, C.E., Saper, C.B., and Elmquist, J.K. 2006. Expression of ghrelin receptor mRNA in the rat and the mouse brain. *J. Comp. Neurol.* **494**:528-548.
13. Berridge, K.C. 1996. Food reward: brain substrates of wanting and liking. *Neurosci. Biobehav. Rev.* **20**:1-25.
14. Wise, R.A. 2002. Brain reward circuitry: insights from unsensed incentives. *Neuron.* **36**:229-240.
15. Richardson, N.R., and Gratton, A. 1998. Changes in medial prefrontal cortical dopamine levels associated with response-contingent food reward: an electrochemical study in rat. *J. Neurosci.* **18**:9130-9138.
16. Blackburn, J.R., Pfau, J.G., and Phillips, A.G. 1992. Dopamine functions in appetitive and defensive behaviours. *Prog. Neurobiol.* **39**:247-279.
17. Berthoud, H.R. 2002. Multiple neural systems controlling food intake and body weight. *Neurosci. Biobehav. Rev.* **26**:393-428.
18. Kelley, A.E. 2004. Ventral striatal control of appetitive motivation: role in ingestive behavior and reward-related learning. *Neurosci. Biobehav. Rev.* **27**:765-776.
19. Saper, C.B., Chou, T.C., and Elmquist, J.K. 2002. The need to feed: homeostatic and hedonic control of eating. *Neuron.* **36**:199-211.
20. Lacey, M.G., Calabresi, P., and North, R.A. 1990. Muscarine depolarizes rat substantia nigra zona compacta and ventral tegmental neurons in vitro through M1-like receptors. *J. Pharmacol. Exp. Ther.* **253**:395-400.
21. Mathon, D.S., et al. 2005. Increased gabaergic input to ventral tegmental area dopaminergic neurons associated with decreased cocaine reinforcement in mu-opioid receptor knockout mice. *Neuroscience.*



- 130:359–367.
22. Johnson, S.W., and North, R.A. 1992. Opioids excite dopamine neurons by hyperpolarization of local interneurons. *J. Neurosci.* **12**:483–488.
23. Pinto, S., et al. 2004. Rapid rewiring of arcuate nucleus feeding circuits by leptin. *Science.* **304**:110–115.
24. Kauer, J.A. 2004. Learning mechanisms in addiction: synaptic plasticity in the ventral tegmental area as a result of exposure to drugs of abuse. *Annu. Rev. Physiol.* **66**:447–475.
25. Naleid, A.M., Grace, M.K., Cummings, D.E., and Levine, A.S. 2005. Ghrelin induces feeding in the mesolimbic reward pathway between the ventral tegmental area and the nucleus accumbens. *Peptides.* **26**:2274–2279.
26. Halem, H.A., et al. 2004. Novel analogs of ghrelin: physiological and clinical implications. *Eur. J. Endocrinol.* **151**(Suppl. 1):S71–S75.
27. Wren, A.M., et al. 2001. Ghrelin causes hyperphagia and obesity in rats. *Diabetes.* **50**:2540–2547.
28. Blackburn, J.R., Phillips, A.G., Jakubovic, A., and Fibiger, H.C. 1989. Dopamine and preparatory behavior: II. A neurochemical analysis. *Behav. Neurosci.* **103**:15–23.
29. Mendoza, J., Angeles-Castellanos, M., and Escobar, C. 2005. Differential role of the accumbens Shell and Core subterritories in food-entrained rhythms of rats. *Behav. Brain Res.* **158**:133–142.
30. Mendoza, J., Angeles-Castellanos, M., and Escobar, C. 2005. Entrainment by a palatable meal induces food-anticipatory activity and c-Fos expression in reward-related areas of the brain. *Neuroscience.* **133**:293–303.
31. Diano, S., et al. 2006. Ghrelin controls hippocampal spine synapse density and memory performance. *Nat. Neurosci.* **9**:381–388.
32. Borgland, S.L., Taha, S.A., Sarti, F., Fields, H.L., and Bonci, A. 2006. Orexin A in the VTA is critical for the induction of synaptic plasticity and behavioral sensitization to cocaine. *Neuron.* **49**:589–601.
33. Narita, M., et al. 2006. Direct involvement of orexinergic systems in the activation of the mesolimbic dopamine pathway and related behaviors induced by morphine. *J. Neurosci.* **26**:398–405.
34. Korotkova, T.M., Sergeeva, O.A., Eriksson, K.S., Haas, H.L., and Brown, R.E. 2003. Excitation of ventral tegmental area dopaminergic and nondopaminergic neurons by orexins/hypocretins. *J. Neurosci.* **23**:7–11.
35. Drazen, D.L., Vahl, T.P., D'Alessio, D.A., Seeley, R.J., and Woods, S.C. 2005. Effects of a fixed meal pattern on ghrelin secretion: evidence for a learned response independent of nutrient status. *Endocrinology.* **147**:23–30.
36. Carr, K.D. 2002. Augmentation of drug reward by chronic food restriction: behavioral evidence and underlying mechanisms. *Physiol. Behav.* **76**:353–364.
37. Leibowitz, S.F., and Hoebel, B.G. 2004. Behavioral neuroscience and obesity. In *The handbook of obesity*. Marcel Dekker. New York, New York, USA. 313–358.
38. Figlewicz, D.P. 2003. Adiposity signals and food reward: expanding the CNS roles of insulin and leptin. *Am. J. Physiol. Regul. Integr. Comp. Physiol.* **284**:R882–R892.
39. Pecina, S., Cagniard, B., Berridge, K.C., Aldridge, J.W., and Zhuang, X. 2003. Hyperdopaminergic mutant mice have higher “wanting” but not “liking” for sweet rewards. *J. Neurosci.* **23**:9395–9402.
40. Orosco, M., and Nicolaidis, S. 1992. Spontaneous feeding-related monoaminergic changes in the rostromedial hypothalamus revealed by microdialysis. *Physiol. Behav.* **52**:1015–1019.
41. Wang, G.J., Volkow, N.D., Thanos, P.K., and Fowler, J.S. 2004. Similarity between obesity and drug addiction as assessed by neurofunctional imaging: a concept review. *J. Addict. Dis.* **23**:39–53.
42. Szczypka, M.S., et al. 1999. Viral gene delivery selectively restores feeding and prevents lethality of dopamine-deficient mice. *Neuron.* **22**:167–178.
43. Szczypka, M.S., et al. 1999. Feeding behavior in dopamine-deficient mice. *Proc. Natl. Acad. Sci. U. S. A.* **96**:12138–12143.
44. Inoue, K., et al. 1993. Scheduled feeding caused activation of dopamine metabolism in the striatum of rats. *Physiol. Behav.* **53**:177–181.
45. Wortley, K.E., et al. 2005. Absence of ghrelin protects against early-onset obesity. *J. Clin. Invest.* **115**:3573–3578. doi:10.1172/JCI26003.
46. Zigman, J.M., et al. 2005. Mice lacking ghrelin receptors resist the development of diet-induced obesity. *J. Clin. Invest.* **115**:3564–3572. doi:10.1172/JCI26002.
47. Langer, F.B., et al. 2005. Sleeve gastrectomy and gastric banding: effects on plasma ghrelin levels. *Obes. Surg.* **15**:1024–1029.
48. Korner, J., et al. 2005. Effects of Roux-en-Y gastric bypass surgery on fasting and postprandial concentrations of plasma ghrelin, peptide YY, and insulin. *J. Clin. Endocrinol. Metab.* **90**:359–365.
49. Cummings, D.E., et al. 2002. Plasma ghrelin levels after diet-induced weight loss or gastric bypass surgery. *N. Engl. J. Med.* **346**:1623–1630.
50. Shuto, Y., et al. 2002. Hypothalamic growth hormone secretagogue receptor regulates growth hormone secretion, feeding, and adiposity. *J. Clin. Invest.* **109**:1429–1436. doi:10.1172/JCI200213300.
51. Wortley, K.E., et al. 2004. Genetic deletion of ghrelin does not decrease food intake but influences metabolic fuel preference. *Proc. Natl. Acad. Sci. U. S. A.* **101**:8227–8232.
52. Horvath, T.L., and Gao, X.B. 2005. Input organization and plasticity of hypocretin neurons: possible clues to obesity's association with insomnia. *Cell Metab.* **1**:279–286.
53. Small, S.V. 1968. Measurement of section thickness. In *Proceedings of the 4th European Congress on Electron Microscopy*. Volume 1. D.S. Bocciarelli, editor. Poliglotta Vaticana. Rome, Italy. 609–610.
54. Keppel, G., and Wickens, T.D. 2004. *Design and analysis: a researcher's handbook*. Prentice Hall. New York, New York, USA. 611 pp.